Electronic Supplementary Material (ESI) for Physical Chemistry Chemical Physics.

Supplementary Material for:
Can reactions follow non-traditional second-order saddle pathways avoiding transition states?

Renuka Pradhan, Upakarasamy Lourderaj*

School of Chemical Sciences
National Institute of Science Education and Research (NISER) Bhubaneswar
HBNI, P. O. Jatni, Khurda, Odisha, India

*To whom correspondence should be addressed; E-mail: u.lourderaj@niser.ac.in.

1 Methods

Ab initio classical trajectory simulations were performed by computing the forces on-the-fly at each step of the trajectory at the CASSCF(4,4)/6-31+G* level of theory [1,2]. The active space for CASSCF(4,4) calculations include both the σ and σ^* orbitals of the C−N bonds. Our earlier investigation on the energetics of the denitrogenation of the **Py** revealed that an active space of (4,4) that involves 4 electrons and the 4 orbitals (2 σ and 2 σ^*) of the C−N bonds captures all the necessary features on the PES depicted by CASPT2 calculations [3]. The correlation of the active orbitals along the synchronous path is given in Fig. S11. The atom labels and definition of the internal coordinates of **Py** used in the manuscript are given in Fig. S12A. The initial coordinates and momenta for the trajectory simulations were selected by using the microcanonical normal mode sampling procedure [4] for given total energy available to the reactant, **Py**. The total amount of energy available to **Py** was calculated by assuming a Boltzmann distribution of states at **TS4f** for the experimental temperature (510.45 K). The total energy available to **Py** can then be expressed as

$$E_{\text{total}} = E_{\text{a}}(\mathbf{TS4f}) + E_{\text{ZPE}} + E_{\text{vib}} + E_{\text{rot}} + RT$$

where, E_{a}(**TS4f**) is the energy of **TS4f** with respect to **Py**, E_{ZPE} is the ZPE of **TS4f**, E_{vib} and E_{rot} are the average vibrational and rotational energies at 510.45 K, and RT is the excess energy given along the reaction coordinate. **TS4f** corresponds to the transition state with the highest energy barrier along the asynchronous path for the denitrogenation reaction. A schematic representation of the total energy available to **Py** with the different components is given in Fig. S12B. The total amount of energy (E_{total}) available to Py from its classical minimum thus calculated was found to be 119.10 kcal/mol. The trajectories were integrated using velocity-Verlet algorithm with a step-size of 0.3 fs. 4000 trajectories were integrated from the reactant region for a maximum of 1.5 ps. It should be pointed that although **Py** and cyclopropane cannot be differentiated as cis and trans, the mechanism of the product formation were followed with respect to the rotation of the terminal methylene groups so that the products (cyclopropane) formed can be compared with the experimental observations for substituted pyrazolines.

In addition, we have also performed trajectory simulations for the ^{15}H isotope substituted 1-pyrazoline (trans-3,5-di-^{15}H-1-pyrazoline) to understand the substituent effect on the mechanisms, dynamics, and product distributions of the denitrogenation reaction. A total of 2500 trajectories were initiated in the reactant region of **DMP** similar to that of **Py** using a microcanonical normal mode sampling procedure. However, in this case we used the same total energy of 119.10 kcal/mol. Increasing the mass lowers the ZPE and results in having a thermal energy corresponding to a temperature of 753 K. This approach was used to increase the reactive trajectories and also to increase the fraction of trajectories following the **SOS** paths.

To understand the post-second-order saddle dynamics of **Py**, we also performed trajectory simulations initiated in the **SOS** region. 300 trajectories were initiated in the **SOS** region, using a microcanonical normal mode sampling procedure with an excess energy of 74.98 kcal/mol at the **SOS** stationary state. A detailed procedure of microcanonical normal mode sampling is given elsewhere[4]. Here we highlight the modification done to accommodate the sampling of a **SOS**. The **SOS** is characterized by $3N-8$ normal modes with positive curvature and 2 modes with negative curvatures of potential energy with respect to the normal mode coordinates. In the sampling method used here, the E_i of energy is assigned randomly to the i^{th} mode of the $3N-8$ normal modes with positive frequencies and random values are chosen for the position Q_i and momentum P_i with random phases. The remaining energy $E = E - \sum E_i$ is also assigned randomly to the rest of the two eigenvectors corresponding to the imaginary frequencies and random coordinates and momenta are chosen with random phases. Finally, the normal mode coordinates and momenta thus chosen are transformed to the Cartesian coordinates and momenta by a linear transformation and the spurious angular momentum arising due to this transformation is added to the molecule. The internal energy obtained from the Cartesian coordinates and momenta are compared to the desired internal energy E and are scaled to agree with in 1%. All the classical trajectory calculations were performed using a modified version of VENUS/NWChem[5,6] on an Intel(R) Xeon(R) CPU E5-2697A v4 @ 2.60GHz computer.

2 Trajectory Analysis

The trajectories were analyzed by following the various internal coordinates of **Py** and **DMP** with time. The atom labels and definition of the internal coordinates are given in Fig. S12A.

(i) Product Distribution: The trajectories were considered as resulting in products when both the C−N distances were at least 10 Å and the three C−C bond distances oscillated about the equilibrium distance of 1.54 Å with the formation of N_2 and **Cp**. The SI, DI, and Ret of configurations for **Cp** were identified by following the dihedral angles (the terminal CH_2 rotations) during the product formation. Of the 314 trajectories, 30 showed isomerization after the initial **Cp** formation. However, for these trajectories we considered the formation of SI, DI, and Ret of products based on the structure for the initial formation of the **Cp**. The distribution of products thus obtained was found to be 128, 116, and 70 trajectories for SI, DI, and Ret of **Cp** respectively. We found that calculating the product distribution by taking the final configuration of the **Cp** (with in the 1.5 ps integration time) for the trajectories showing isomerization also gave a similar product distribution. The distribution was found to be 128, 114, and 72 trajectories for SI, DI, and Ret of **Cp** respectively.

(ii) Synchronous vs asynchronous pathways: The mechanism followed by each trajectory was characterized by following a few relevant internal coordinates as a function of time. To characterize if the trajectories followed the synchronous or asynchronous path, we followed both C−N distances with time. A synchronous path involved a simultaneous breaking of the C−N bonds during the dissociation. The trajectories were categorized as following the synchronous path if the time difference between both the C−N bond distances attaining a value of 2.5 Å is less than one vibrational period of C−N stretching (40 fs). The value of 2.5 Å corresponds to the upper limit of the C−N bond distances defining the **TS1** region. The **TS1** region was defined as the range of C−N bond distances sampled in a microcanonical procedure[4] at the **TS1**. This range was found to be 1.7 to 2.5 Å.

(ii) Product energies: For the computation of the product energies, we considered only those trajectories that conserved the total energy until the C−N bond distances were at least 15 Å. This number was 164 and 105 for synchronous and asynchronous trajectories respectively amounting to about 85% of the reactive trajectories. The relative translational energies and the rotational energies of the products **Cp** and N_2 were computed using standard methods described elsewhere[7].

(iii) Fragment energies along the reaction paths: The relative kinetic energies and the rotational energies of the **Cp** and N_2 fragments during the dissociation process were also computed from the momenta of the respective atoms of the fragments[7]. These give details about the change in the individual rotational and translational energy components of the kinetic energies during the bond breaking. The average of the relative translational and rotational energies of the trajectories at fixed values of d_S were also computed.

(iv) Diradical lifetimes: We computed the lifetime of a radical defined as the time the molecule exhibits a diradical character. The electron densities of the HOMO and LUMO were followed during the dissociation process and the system was considered to be a diradical if the electron density of the LUMO had a value between 0.45 and 1.55. In the case of the asynchronous paths, the system is expected to go through both the **DZ** and **TMD** diradicals. They were differentiated by following the C−N distances. The diradical formed after both the C−N distances become 4.5 Å was considered to be **TMD**. This value was chosen since the largest C−N distance corresponding to the **TSs** along the asynchronous paths was about 4.5 Å.

(v) Second-order saddle trajectories: To identify the trajectories following the SO path, a set of combined coordinates $\phi_S = (\phi_1 - \phi_8)/2$ and $d_S = (d_1 + d_2)/2$ were identified and a PES was mapped by performing a relaxed scan for fixed values of ϕ_S and d_S $(= d_1 = d_2)$. ϕ_S and d_S also faithfully represent the PES covering the stationary points along the synchronous denitrogenation path. An **SOS** region was identified from the values of the coordinates ϕ_1, ϕ_8, d_1, and d_2 sampled in the trajectories initiated at the **SOS** region using a microcanonical procedure. This resulted in a number of trajectories passing through the **SOS** region, however recrossing to the reactant region. Hence, the ϕ_1, ϕ_8, d_1, and d_2 coordinates were adjusted to avoid recrossing trajectories and also maximize the trajectories following the **SOS** path. The **SOS** region was thus defined as the range d_1 or $d_2 = 2.02$ to 2.18 Å and $\phi_S = -18°$ to 18°.

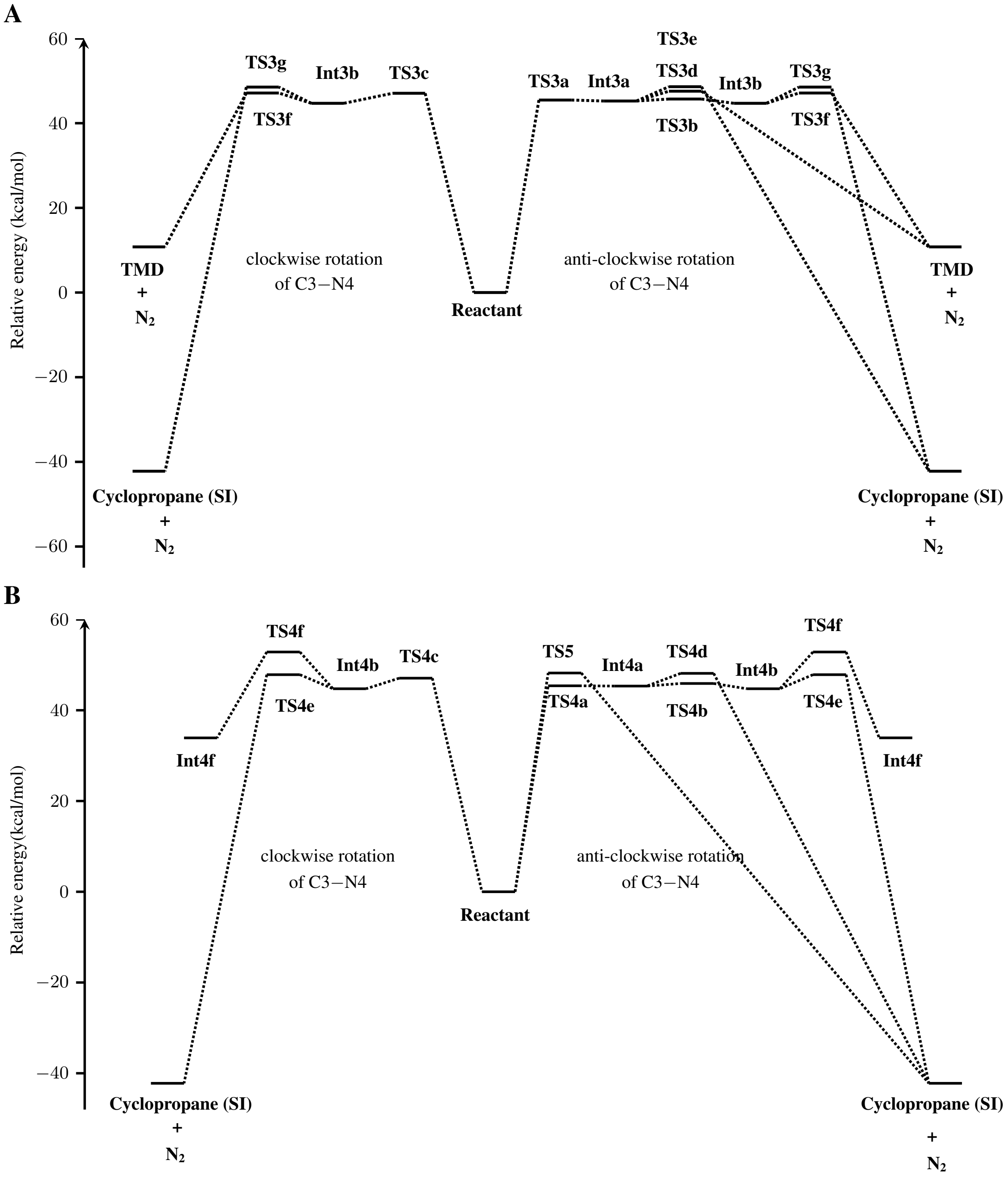

Fig. S1: Potential energy profiles for the asynchronous pathways through (**A**) planar-like and (**B**) perpendicular-like diazenyl diradicals in the thermal denitrogenation of 1-pyrazoline obtained at CASSCF(4,4)/6-31+G* level of theory. The path through **TS5** corresponds to a concerted asynchronous path. Reproduced from Ref.[3] with permission from the Royal Society of Chemistry.

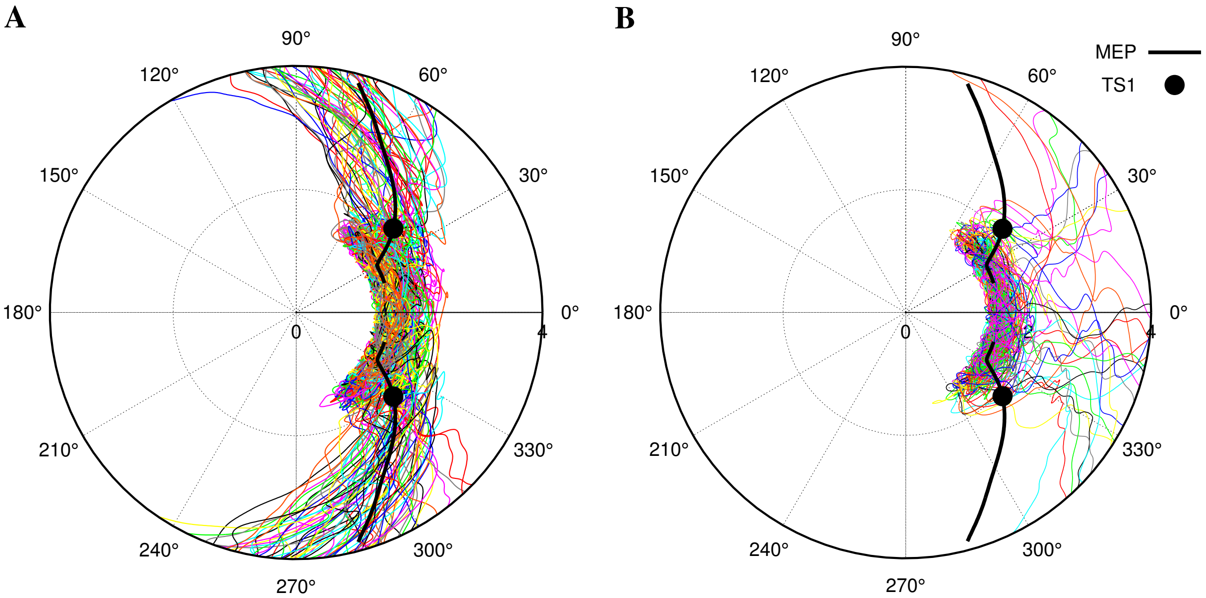

Fig. S2: Plots of ∠C1C2C3N4 and ∠C3C2C1N5 (°) vs C3−N4 distance (Å) for representative trajectories that (**A**) follow MEP and (**B**) do not follow MEP.

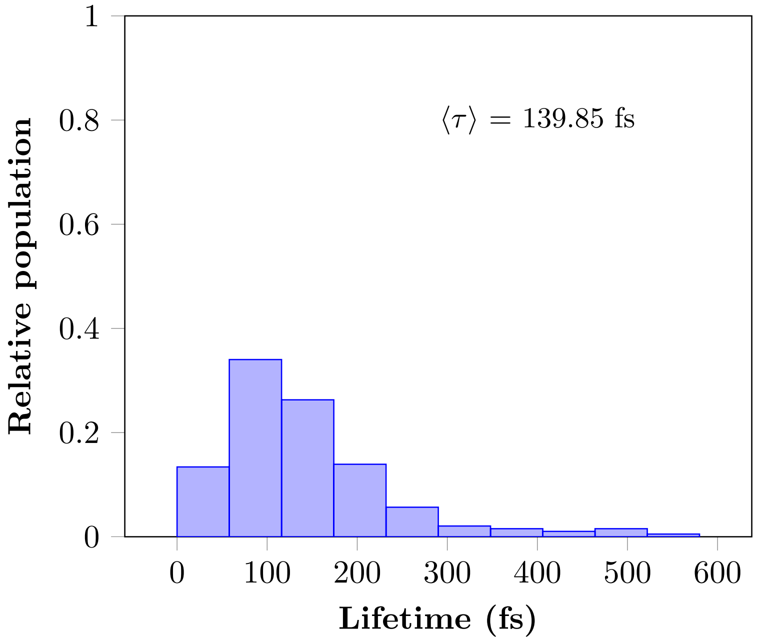

Fig. S3: Lifetime distribution of **TMD** obtained for the synchronous trajectories. The average lifetime $\langle \tau \rangle$ of **TMD** intermediate was found to be 139.85 fs.

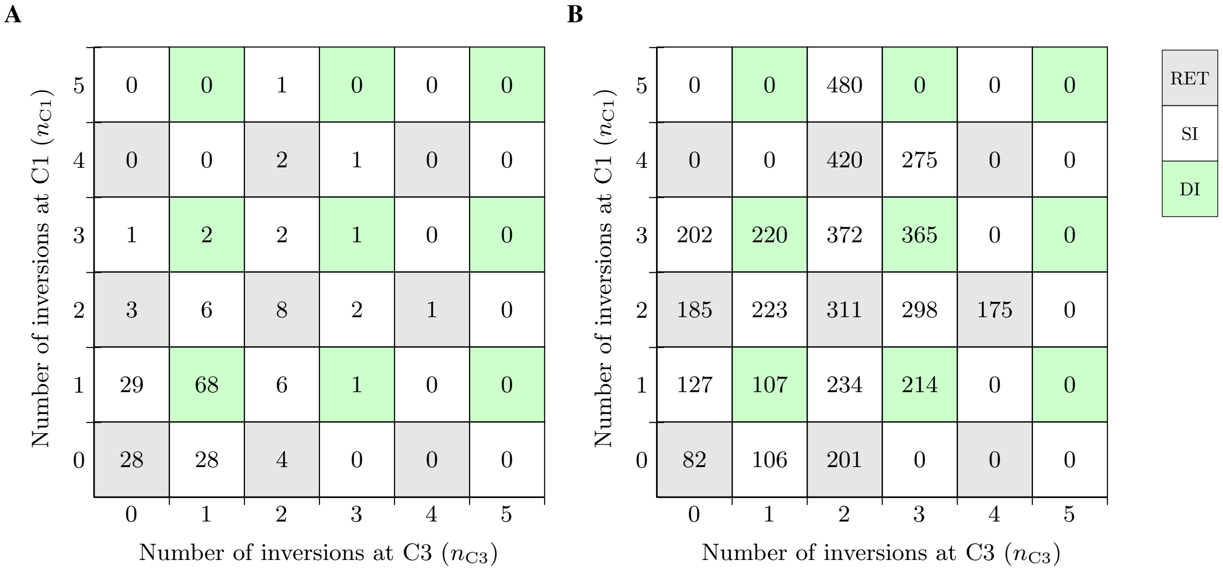

A

	0	1	2	3	4	5
5	0	0	1	0	0	0
4	0	0	2	1	0	0
3	1	2	2	1	0	0
2	3	6	8	2	1	0
1	29	68	6	1	0	0
0	28	28	4	0	0	0

B

	0	1	2	3	4	5
5	0	0	480	0	0	0
4	0	0	420	275	0	0
3	202	220	372	365	0	0
2	185	223	311	298	175	0
1	127	107	234	214	0	0
0	82	106	201	0	0	0

Fig. S4: Matrix representing (**A**) the number of trajectories showing (n_{C1}, n_{C3}) inversions at the C1 and C3 atoms respectively, (**B**) average lifetime (fs) of the **TMD**s for each (n_{C1}, n_{C3}) inversions. For example, a value of 107 fs corresponds to the average lifetime for 68 trajectories showing (1,1) inversions, i.e. one inversion each at the C1 and C3 terminal atoms. The type of products obtained is given in the color code.

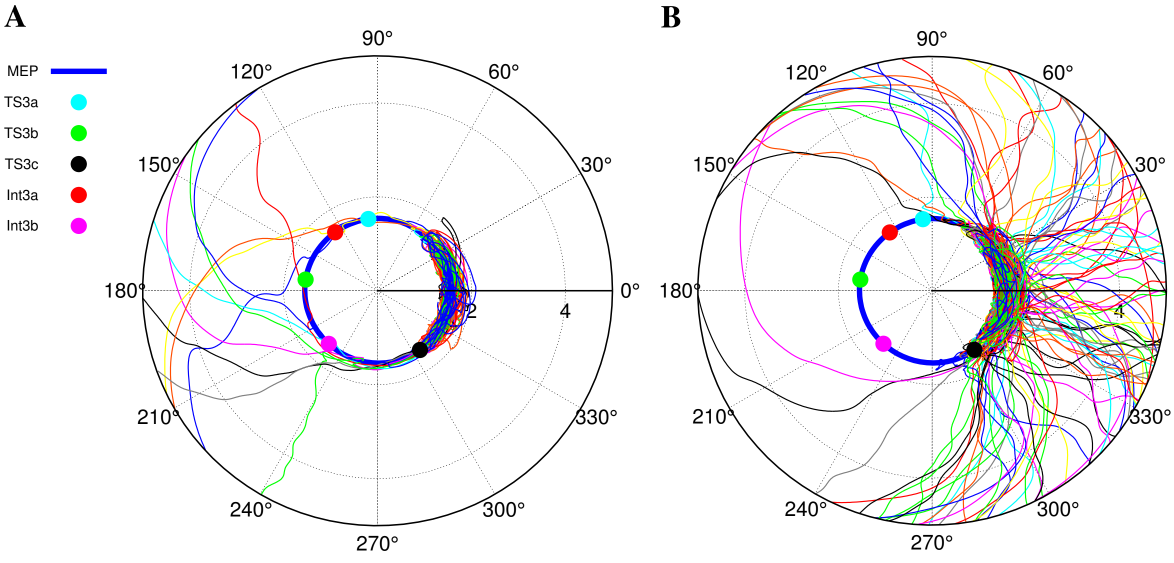

Fig. S5: Plots of ∠C2-C3-N4-N5 (°) vs C3−N4 (Å) or ∠C2-C1-N5-N4 (°) vs C1−N5 (Å) distance for the asynchronous trajectories that (**A**) follow MEP and (**B**) do not follow MEP. ∠C2-C3-N4-N5 vs C3−N4 is plotted if C1−N5 bond breaks first and ∠C2-C1-N5-N4 vs C1−N5 is plotted if C3−N4 is broken first.

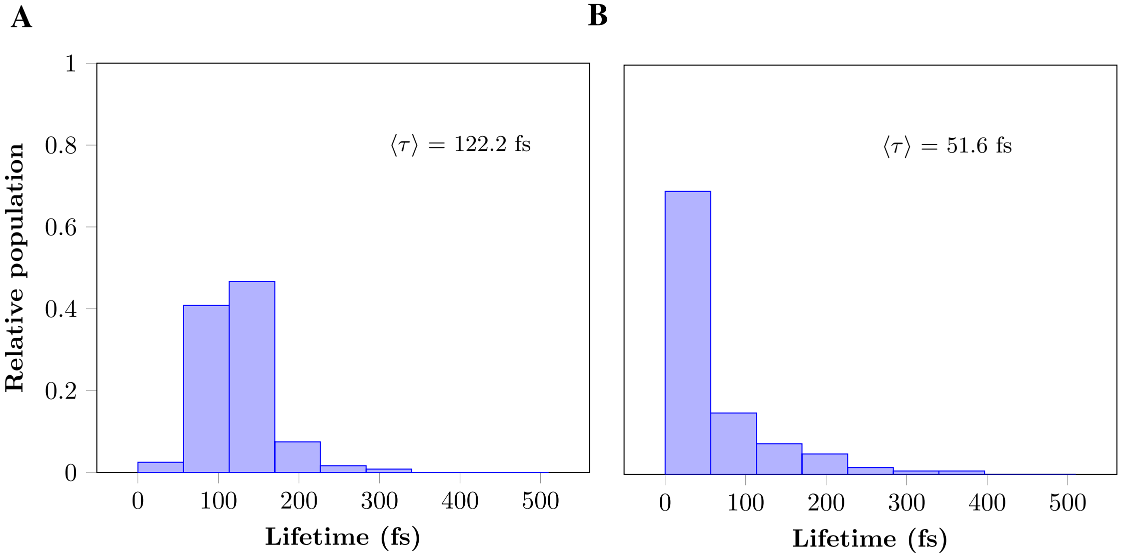

Fig. S6: Lifetime distribution of (**A**) **DZ** and (**B**) **TMD** obtained for the asynchronous trajectories for 1-pyrazoline. The average lifetimes $\langle\tau\rangle$ of **DZ** and **TMD** were found to be 122.2 and 51.6 fs respectively.

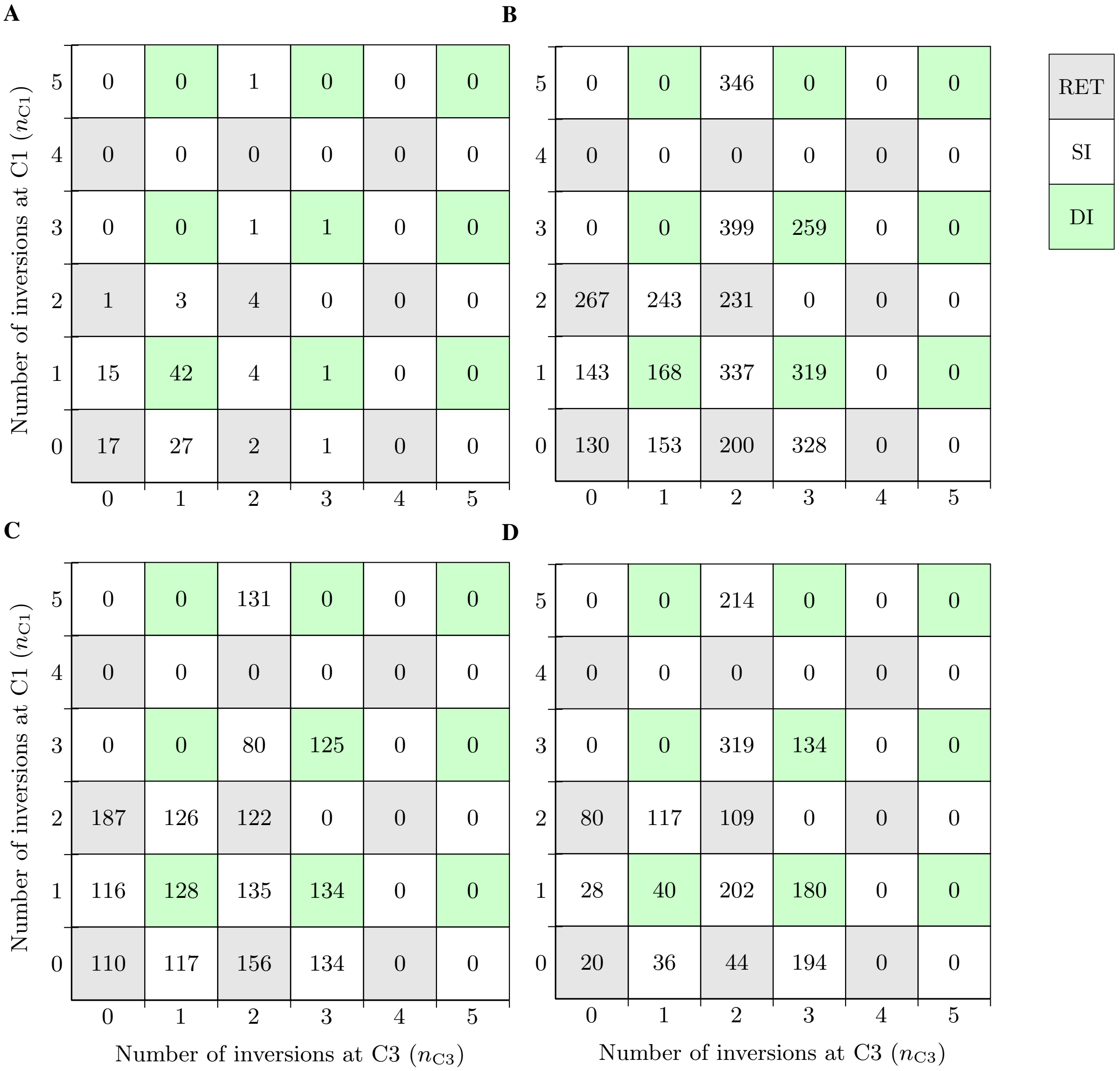

A

	0	1	2	3	4	5
5	0	0	1	0	0	0
4	0	0	0	0	0	0
3	0	0	1	1	0	0
2	1	3	4	0	0	0
1	15	42	4	1	0	0
0	17	27	2	1	0	0

B

	0	1	2	3	4	5
5	0	0	346	0	0	0
4	0	0	0	0	0	0
3	0	0	399	259	0	0
2	267	243	231	0	0	0
1	143	168	337	319	0	0
0	130	153	200	328	0	0

C

	0	1	2	3	4	5
5	0	0	131	0	0	0
4	0	0	0	0	0	0
3	0	0	80	125	0	0
2	187	126	122	0	0	0
1	116	128	135	134	0	0
0	110	117	156	134	0	0

D

	0	1	2	3	4	5
5	0	0	214	0	0	0
4	0	0	0	0	0	0
3	0	0	319	134	0	0
2	80	117	109	0	0	0
1	28	40	202	180	0	0
0	20	36	44	194	0	0

Fig. S7: Matrix representing (**A**) the number of trajectories showing (n_{C1}, n_{C3}) inversions at the C1 and C3 atoms, (**B**) average lifetimes (fs) of the total diradical (**TMD** + **DZ**), (**C**) average lifetimes (fs) of **DZ**, and (**D**) average lifetimes (fs) of **TMD** for each (n_{C1}, n_{C3}) inversions.

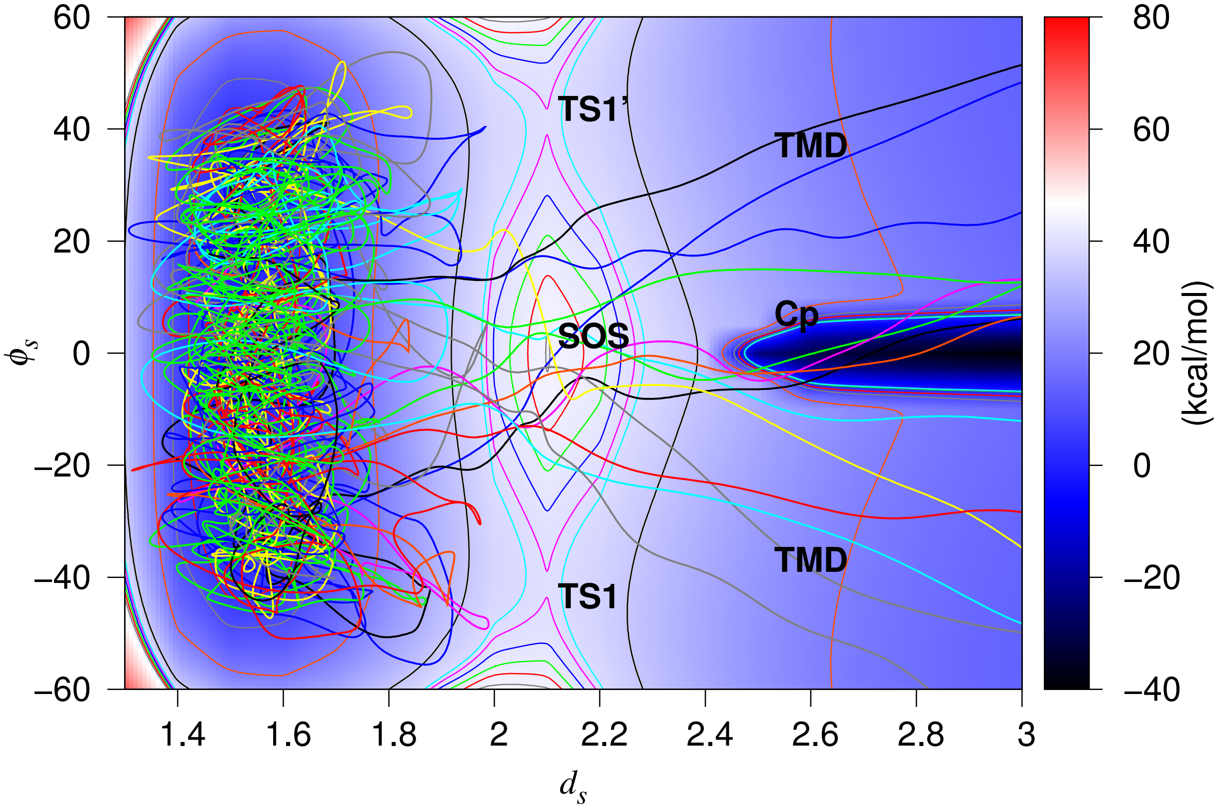

Fig. S8: Plot of ϕ_S (°) and d_S (Å) for 14 trajectories projected on the relaxed PES for the synchronous denitrogenation path obtained for 1-pyrazoline. The trajectories form cyclopropane from the reactants passing through the **SOS** region.

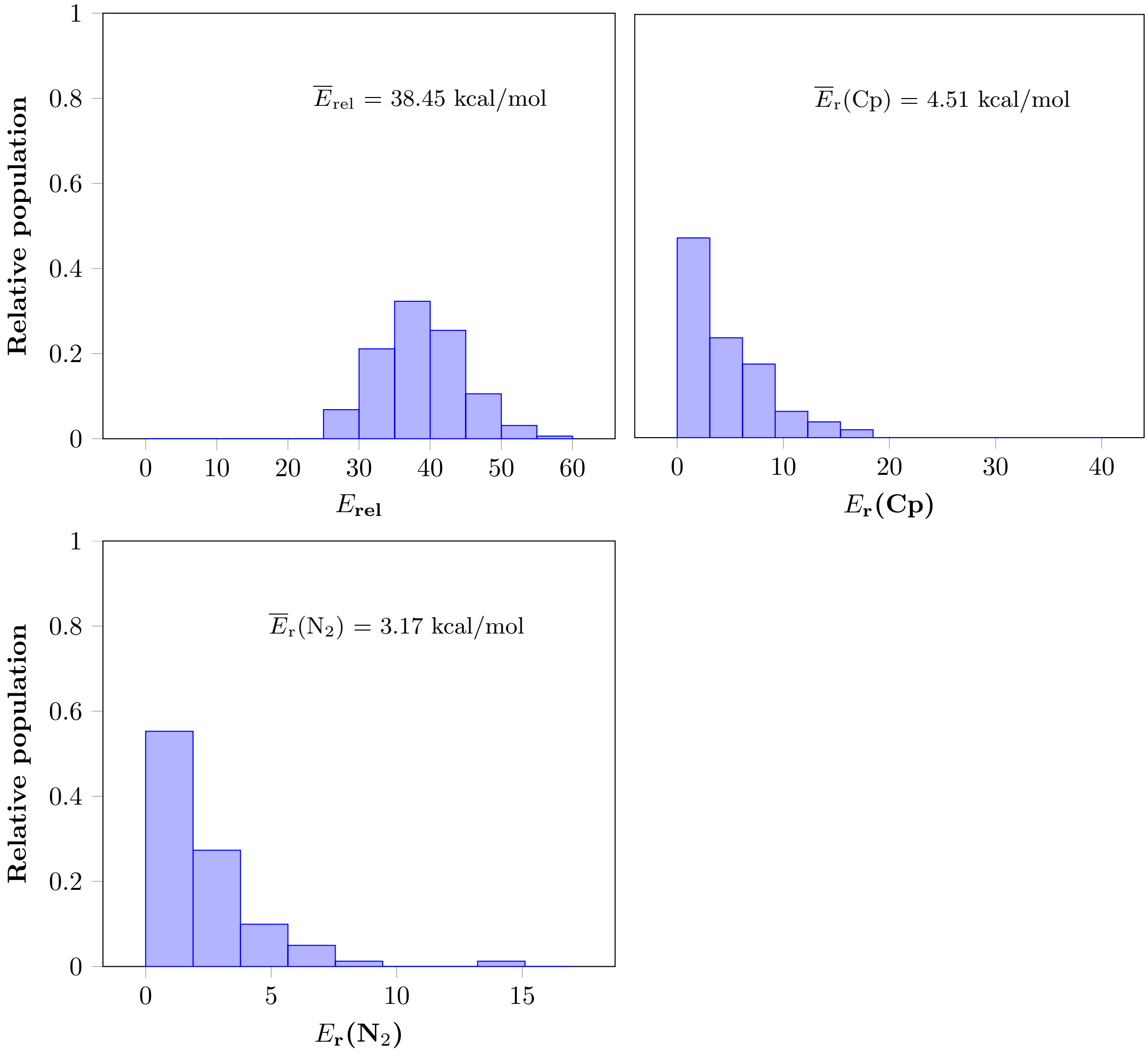

Fig. S9: Distributions of product energies (kcal/mol) obtained for the synchronous trajectories for 1-pyrazoline. The average energies $\overline{E}_{\mathrm{rel}}$, $\overline{E}_{\mathrm{r}}(\mathrm{Cp})$, and $\overline{E}_{\mathrm{r}}(\mathrm{N}_2)$ were found to be 38.45, 4.51, and 3.17 kcal/mol respectively.

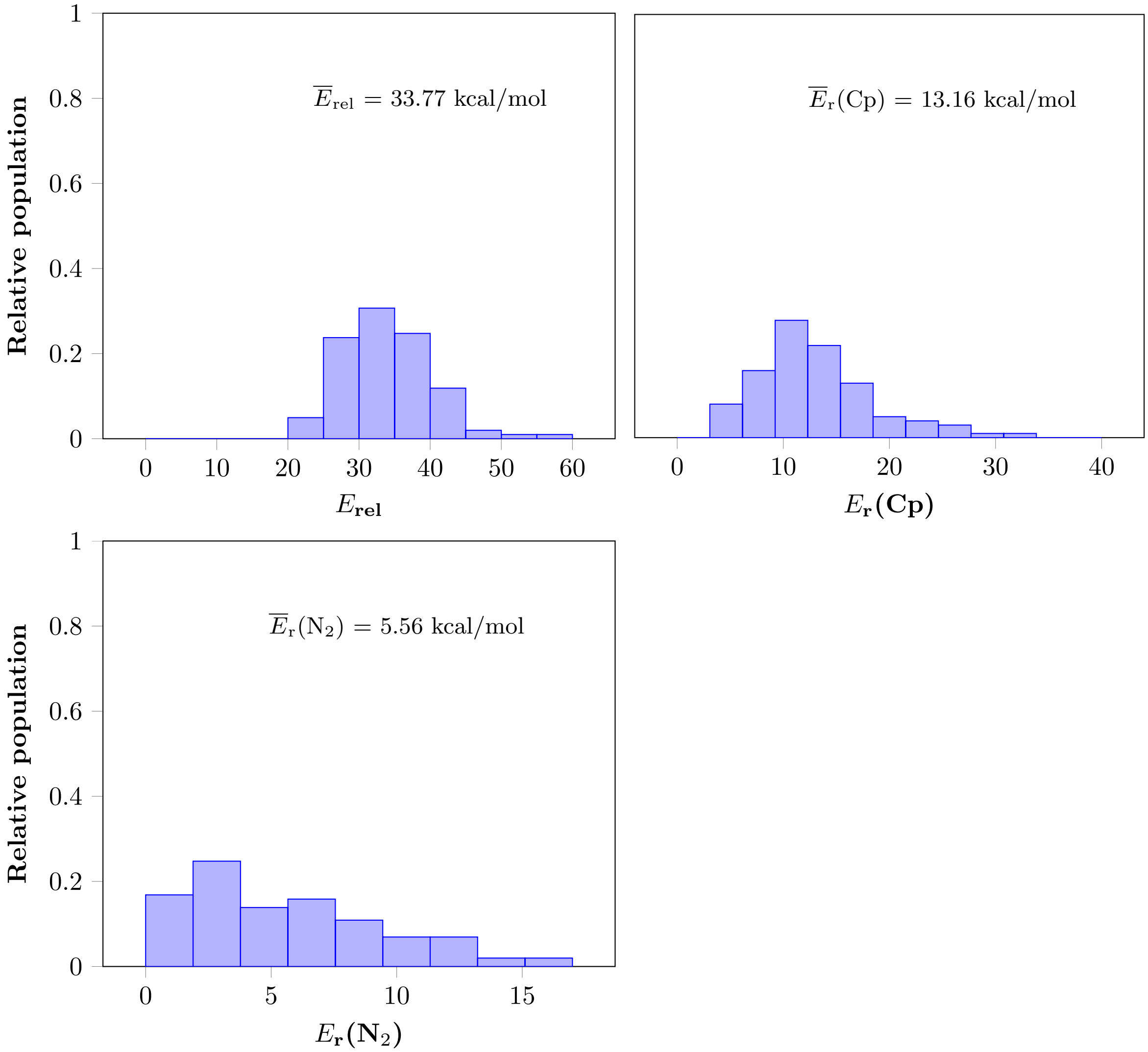

Fig. S10: Distribution of product energies (kcal/mol) obtained for the asynchronous trajectories for 1-pyrazoline. The average energies $\overline{E}_{\text{rel}}$, $\overline{E}_{\text{r}}(\text{Cp})$, and $\overline{E}_{\text{r}}(\text{N}_2)$ were found to be 33.77, 13.16, and 5.56 kcal/mol respectively.

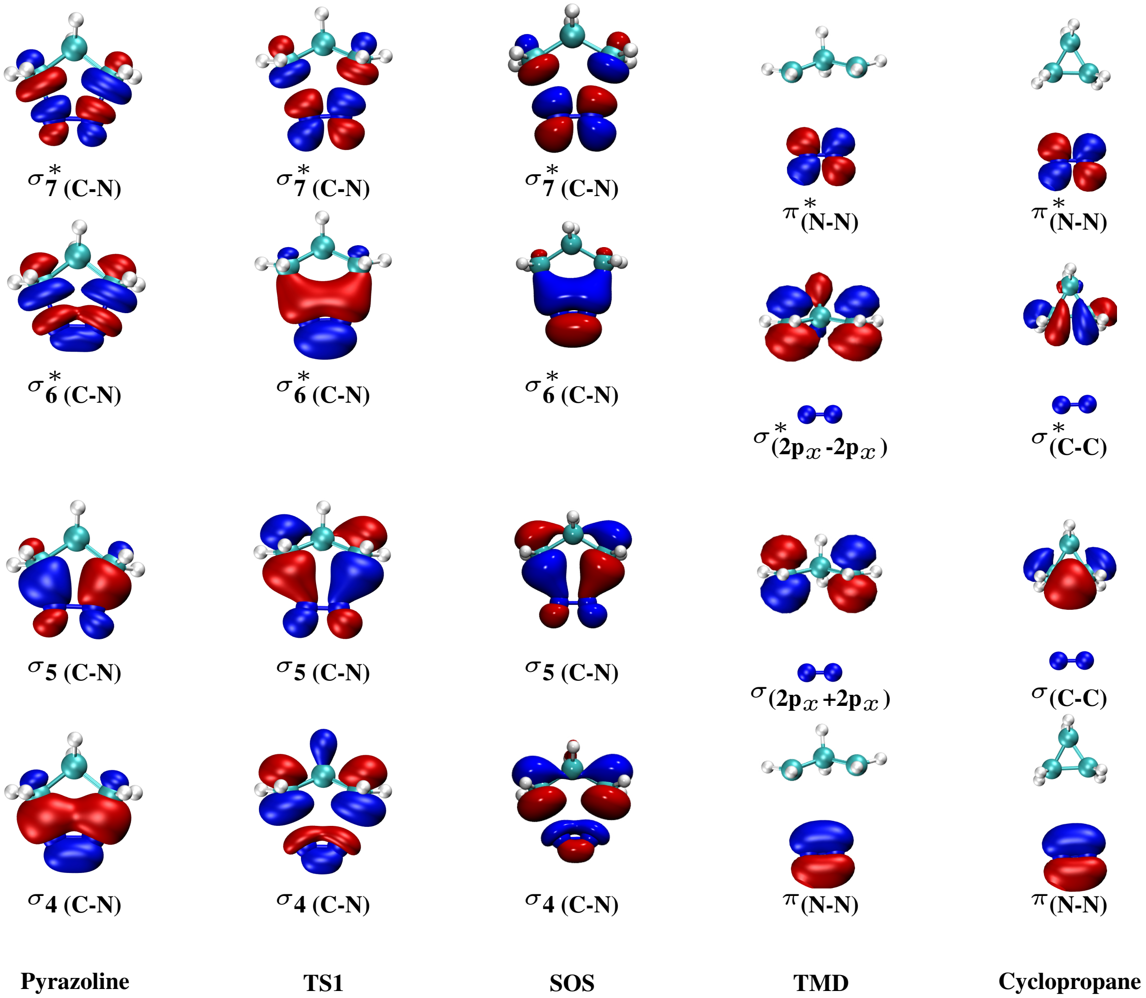

Fig. S11: Correlation diagram of active-space orbitals along the synchronous denitrogenation path from 1-pyrazoline to **TMD** and cyclopropane formation.

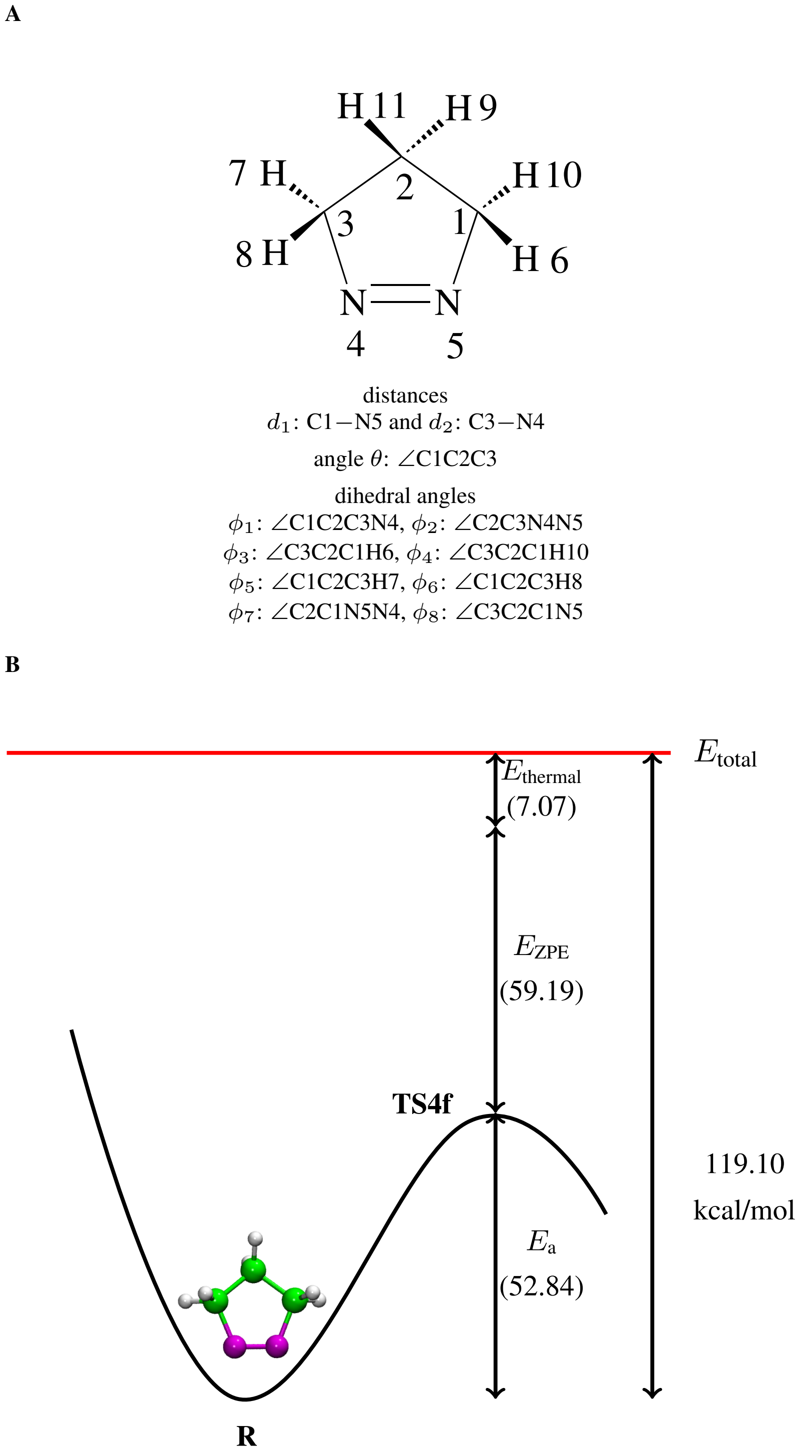

Fig. S12: Schematic diagram representing (**A**) the atom labels and atom numbers for 1-pyrazoline and important geometrical parameters considered in the present study and (**B**) decomposition of the total energy available to the system in the trajectory simulations ($E_{\text{thermal}} = E_{\text{vib}} + E_{\text{rot}} + RT$).

References

[1] B. O. Roos, *Adv. Chem. Phys.*, 1987, **69**, 399–445.

[2] W. Hehre, L. Radom, P. v. R. Schleyer and J. Pople, *Ab initio molecular orbital theory*, Wiley: New York, 1986.

[3] R. Pradhan and U. Lourderaj, *Phys. Chem. Chem. Phys.*, 2017, **19**, 27468–27477.

[4] W. L. Hase, *Encyclopedia of Computational Chemistry*, 2002, **1**, 402–407.

[5] U. Lourderaj, R. Sun, S. C. Kohale, G. L. Barnes, W. A. de Jong, T. L. Windus and W. L. Hase, *Comput. Phys. Commun.*, 2014, **185**, 1074–1080.

[6] M. Valiev, E. Bylaska, N. Govind, K. Kowalski, T. Straatsma, H. V. Dam, D. Wang, J. Nieplocha, E. Apra, T. Windus and W. de Jong, *Comput. Phys. Commun.*, 2010, **181**, 1477–1489.

[7] W. L. Hase, *Encyclopedia of Computational Chemistry*, 2002, **1**, 399–402.